Negative-angle refraction and reflection of visible light with a planar array of silver dimers

Sergey Belan,[1,2*] **Vladimir Parfenyev,**[2] **and Sergey S. Vergeles**[2]

[1]*Moscow Institute of Physics and Technology, Institutskiy per. 9, 141700, Dolgoprudny, Russia*
[2]*Landau Institute for Theoretical Physics RAS, Kosygina 2, 119334, Moscow, Russia*

[*]*sergb27@yandex.ru*

Abstract: We study the plane wave scattering on a planar periodic array of silver dimers. It is found that an appropriately designed array provides the sharp turn of TE-polarized incident beam in orthogonal (opposite) directions through the effects of negative-angle refraction (reflection).

OCIS codes: (050.1950) Diffraction gratings; (050.6624) Subwavelength structures; (130.4815) Optical switching devices.

References and links

1. N. Yu and F. Capasso, "Flat optics with designer metasurfaces," Nature Materials **13**, 139–150 (2014).
2. N. Yu, P. Genevet, M. A. Kats, F. Aieta, J.-P. Tetienne, F. Capasso, and Z. Gaburro, "Light propagation with phase discontinuities: generalized laws of reflection and refraction," Science **334**, 333–337 (2011).
3. X. Ni, N. K. Emani, A. V. Kildishev, A. Boltasseva, and V. M. Shalaev, "Broadband light bending with plasmonic nanoantennas," Science **335**, 427–427 (2012).
4. S. Sun, K.-Y. Yang, C.-M. Wang, T.-K. Juan, W. T. Chen, C. Y. Liao, Q. He, S. Xiao, W.-T. Kung, G.-Y. Guo *et al.*, "High-efficiency broadband anomalous reflection by gradient meta-surfaces," Nano Lett. **12**, 6223–6229 (2012).
5. J. Du, Z. Lin, S. Chui, W. Lu, H. Li, A. Wu, Z. Sheng, J. Zi, X. Wang, S. Zou *et al.*, "Optical beam steering based on the symmetry of resonant modes of nanoparticles," Phys. Rev. Lett. **106**, 203903 (2011).
6. A. Wu, H. Li, J. Du, X. Ni, Z. Ye, Y. Wang, Z. Sheng, S. Zou, F. Gan, X. Zhang *et al.*, "Experimental demonstration of in-plane negative-angle refraction with an array of silicon nanoposts," Nano Lett. **15**, 2055–2060 (2015).
7. A. Ivanov, A. Shalygin, V. Lebedev, P. Vorobev, S. Vergiles, and A. Sarychev, "Plasmonic extraordinary transmittance in array of metal nanorods," Appl. Phys. A **107**, 17–21 (2012).
8. P. B. Johnson and R.-W. Christy, "Optical constants of the noble metals," Phys. Rev. B **6**, 4370 (1972).
9. B. Lukyanchuk and V. Ternovsky, "Light scattering by a thin wire with a surface-plasmon resonance: Bifurcations of the poynting vector field," Phys. Rev. B **73**, 235432 (2006).
10. J. Kottmann and O. Martin, "Plasmon resonant coupling in metallic nanowires," Opt. Express **8**, 655–663 (2001).
11. P. Vorobev, "Electric field enhancement between two parallel cylinders due to plasmonic resonance," Journal of Experimental and Theoretical Physics **110**, 193–198 (2010).
12. V. E. Babicheva, S. S. Vergeles, P. E. Vorobev, and S. Burger, "Localized surface plasmon modes in a system of two interacting metallic cylinders," JOSA B **29**, 1263–1269 (2012).
13. S. Belan and S. Vergeles, "Plasmon mode propagation in array of closely spaced metallic cylinders," Opt. Mater. Express **5**, 130–141 (2015).

1. Introduction

Manipulation of optical wavefront at nanoscale is one of the central problem of modern photonics. Recent remarkable progress in this field is largely due to implementation of the phase gradient meta-surfaces [1] which are the two-dimensional arrays of subwavelength antennas with spatially varying geometric parameters (shape, size, orientation). The complex structure

#251351 Received 5 Oct 2015; revised 12 Nov 2015; accepted 12 Nov 2015; published 18 Nov 2015

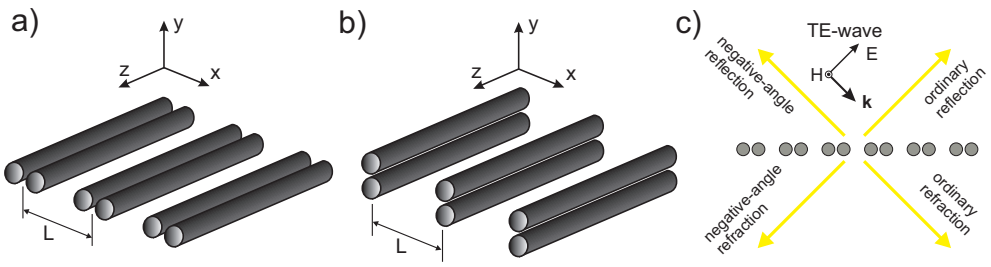

Fig. 1. Periodic array of cylinder dimers with longitudinal (a) and transversal (b) orientation of unit cell. (c): TE-wave scattering on array of pairs of nanocylinders in the case $L = \lambda/\sqrt{2}$, $\theta = 45^\circ$. The yellow arrows schematically indicate the permitted directions of the outgoing waves, which correspond to the 0th and -1st diffraction orders.

of the unit cell of such array introduces a spatially varying phase response with subwavelength resolution, allowing, for example, controllable refraction and reflection of the incident light beam in anomalous directions [2–4].

The extraordinary optical properties of the periodic scattering structure do not necessarily imply the complex design of its elemental cell. Say, the negative directional transmission of an incident beam has been recently demonstrated both numerically and experimentally in the near-infrared regime with a regular chain of identical silicon nanorods [5, 6]. The effect is observed near the dipolar resonance of individual rods provided that the induced dipole moments in adjacent rods have a phase difference of π. In this work, we show that similar scheme of beam steering allows to manipulate the optical wavefront in visible regime when the metal rods are used instead of dielectric ones. Specifically, we consider a periodic planar (2d) array with unit cell consisting of a pair of infinitely long metal cylinders. Analysis includes the cases of both longitudinal and transversal orientation of dimers with respect to the direction of system periodicity, see Fig. 1. It is demonstrated that the ultrathin array of longitudinally orientated dimers can refract an incident TE-wave in a negative way, whereas the transversal dimers' orientation under certain conditions leads to phenomenon of negative reflection. These phenomena are associated with the resonance excitation of strongly localized plasmonic modes in the inter-cylinders gaps [7]. Noteworthy, the efficiency of the anomalous beam redirection is restricted only by ohmic losses in metal and can reach 100% in the idealized limit of dissipation-free dimers. Our results can lead to applications in designing of ultra-compact optical components in photonic circuits.

We use the COMSOL Multiphysics package for full scale electrodynamic simulations of plane wave scattering on an array of silver dimers. The silver is chosen for the role of plasmonic material because of its relatively small losses at optical frequencies. The complex dielectric permittivity of silver is extracted from tabulated empirical data [8].

2. Plasmonic resonances of cylinder dimer

The metal nanoparticles are known to exhibit strong response to external electromagnetic field at specific frequencies due to excitation of plasmonic resonances. When the particle size is much smaller than illumination wavelength λ, the resonance condition stems mainly from the λ-dependence of the dielectric permittivities ε_m and ε_d for the metal and the surrounding dielectric media correspondingly. In particular, the resonance condition for lowest (dipolar) mode of a single metal cylinder with subwavelength diameter writes simply $\varepsilon_m/\varepsilon_d = -1$ [9]. In the case of silver nanorod embedded in air one has $\mathrm{Re}\,\varepsilon_m = -1$ at $\lambda \approx 340$ nm so that the resonance lies in the ultra-violet region.

#251351 Received 5 Oct 2015; revised 12 Nov 2015; accepted 12 Nov 2015; published 18 Nov 2015

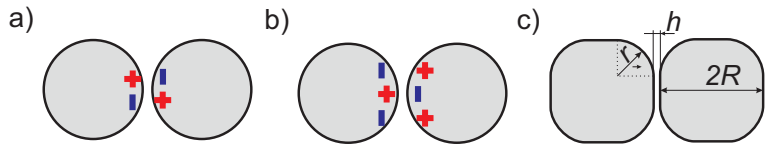

Fig. 2. A sketch of the electrical charge distribution for the two lowest plasmonic modes which are magnetic dipole (a) and electric dipole (b) oscillations in a pair of closely spaced cylinders. (c) The dimer consisting of metal rods with quasi-square cross section.

Large optical response in visible part of spectrum can be obtained by introducing the coupling between silver nanoparticles. A pair of closely spaced metal cylinders (dimer) exhibits strongly red-shifted plasmonic resonances when it is excited by external electric field oriented normally to cylinders' axes [10]. The electromagnetic field of the corresponding plasmonic excitations turns to be concentrated mainly inside the gap between cylinders. Figs. 2(a) and 2(b) illustrate schematically the distribution of polarization charges at the metallic boundaries for two lowest plasmonic modes of cylinder dimer. For the dimer dimensions much smaller than the wavelength of incident light, the resonance condition for these modes is found to be [11]

$$\frac{\varepsilon_m(\lambda)}{\varepsilon_d} = -\frac{h+2R}{\sqrt{h(h+4R)}}, \tag{1}$$

where R is the radius of the cylinders and h is the separation between their surfaces. At $h \gg R$ one obtains $\varepsilon_m/\varepsilon_d \approx -1$ that corresponds to the dipolar resonances of uncoupled cylinders [9]. The opposite limit of nearly touching cylinders gives $\varepsilon_m/\varepsilon_d \approx -\sqrt{R/h}$. By changing the ratio R/h one can set the resonance at desired frequency.

As it is shown in [12], for nearly touching cylinders the electrostatic estimate (1) works fairly well even when the wavelength λ of incident light is of order of R. The reason is that the electromagnetic field is strongly localized inside the gap region at scales $\sim \sqrt{hR}$.

3. Negative-angle refraction and reflection

Being periodically arranged in an array, the dimers act as secondary sources of electromagnetic waves. Inspired by the setup proposed in [5], we consider the scattering scenarios in which the neighbouring unit cells are excited in anti-phase. Namely, we assume that (I) period of the array is $L = \lambda/\sqrt{2}$, where λ is the wavelength of incident plane wave, and (II) the incident angle is $\theta = 45^\circ$. Then, the induced gap charge oscillations in adjacent dimers have a phase difference of π. It is easy to see that the given structure can be viewed as a diffraction grating, which simultaneously supports the 0th and -1st order refraction and reflection, see Fig. 1(c). The ordinary (positive-angle) refraction and reflection are corresponding to 0th order diffraction channels, while anomalous (negative-angle) refraction and reflection are corresponding to -1st order channels.

The focus of the study is on the case where the E field of the incident wave is polarized normally to axes of cylinders and H field is parallel to axes. Just this polarization excites the resonances inside the intercylinder gap. Considering the grid as a whole, the polarization should be called p-polarization, whereas it is TE-wave for each pair of cylinders. Numerical modelling indicates that at $\lambda = 440$ nm, $L = \lambda/\sqrt{2}$, $R = 53$ nm and $h = 1.9$ nm the ordinary reflection and refraction and the anomalous reflection are strongly suppressed so that only -1st order refraction is left. This is an essence of the negative-angle refraction phenomenon: the refracted beam lies on the same side of the normal as the incident beam, see Fig. 3(a). The anomalously refracted wave carries 73% of energy of the impinging wave, while the other diffracted

#251351 Received 5 Oct 2015; revised 12 Nov 2015; accepted 12 Nov 2015; published 18 Nov 2015

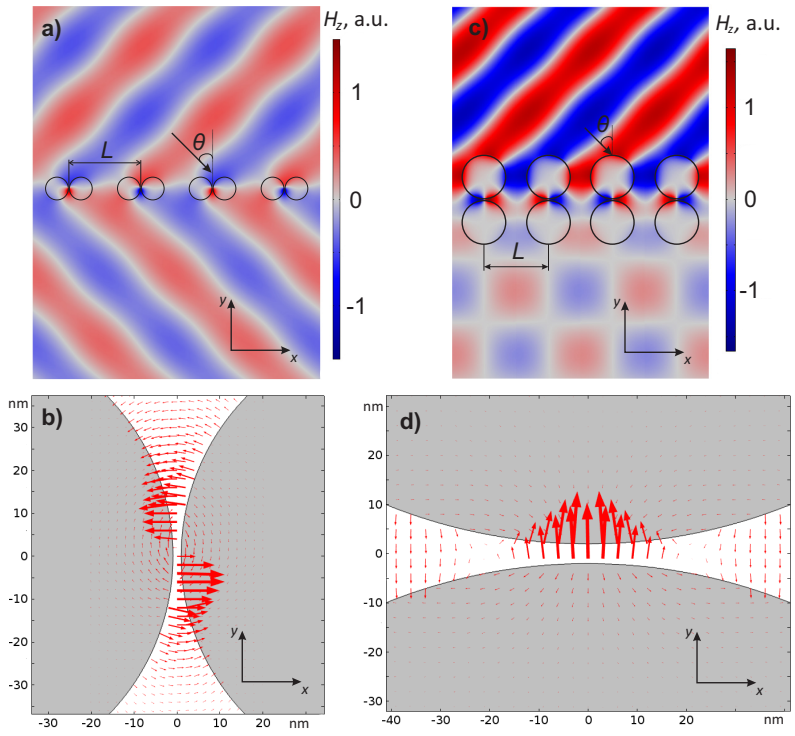

Fig. 3. (a) and (c): The distribution of H_z-component demonstrates the negative-angle refraction and reflection phenomena. Neighbouring dimers are exited in anti-phase. (b) and (d): The corresponding distribution of electric field in the gap region. Excited modes are the lowest plasmonic modes in dimer, see Figs. 2(a) and 2(b).

waves only have 5% at sum. Despite the small loss tangent of silver at the chosen frequency ($tg \sim 0.03$), the system suffers from quite large energy losses which arise because of dramatic enhancement of the induced electric field in the gap regions. Note that efficiency of negative-angle refraction becomes 97% when one sets the complex part of metal permittivity to be zero while keeping all other parameters unchanged.

The spatial distribution of the electric field in the gap region is shown in Fig. 3(b). We thus conclude that anomalous negative-angle refraction is associated with the excitation of lowest transversal mode of the dimers which corresponds to magnetic dipole oscillations, see Fig. 2(a). The magnetic dipole moment is directed along the axes of cylinders.

The angle resolved scattering spectra is plotted in Fig. 4(a) and it shows that the anomalous refraction can be achieved over a wide range of incident angles, varying from 30° to 70°. Note that if $\theta < \arcsin(\sqrt{2}-1) \approx 25°$ then -1st order refraction channel disappears and negative-angle transmission becomes impossible.

At $\lambda = 440$ nm the choice $h = 1.9$ nm, $R = 53$ nm is optimal for silver dimers, i.e. it provides the maximum efficiency of negative transmission. As the field frequency goes down, the optimal gap width decreases, while the optimum radius increases. Say, at $\lambda = 490$ nm the optimum gap becomes just $h = 1.1$ nm and the optimum radius is $R = 62$ nm, that provides the efficiency 69%. In Table 1 the optimal geometrical parameters and the resulting efficiency are presented for a range of wavelength. Note that in all cases the grating structure is much thinner than the operational wavelength.

#251351 Received 5 Oct 2015; revised 12 Nov 2015; accepted 12 Nov 2015; published 18 Nov 2015

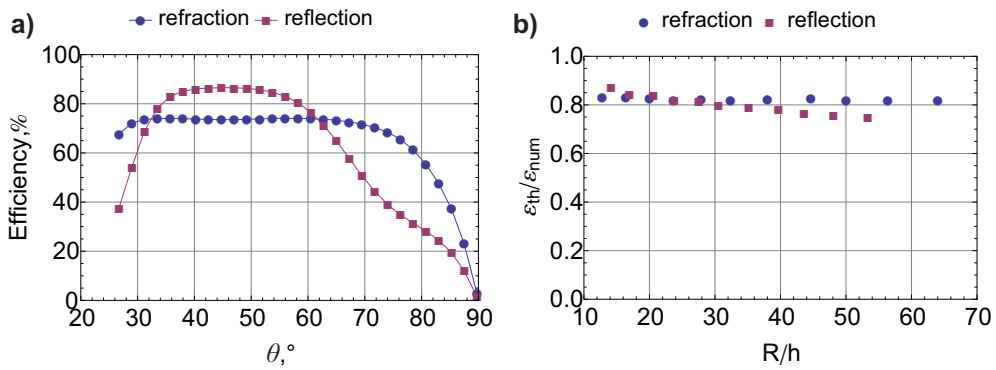

Fig. 4. (a) The efficiency of negative-angle refraction (reflection) as a function of incidence angle θ for the following parameters: $\lambda = 440$ nm, $L = \lambda/\sqrt{2}$, $R = 53$ nm and $h = 1.9$ nm ($\lambda = 440$ nm, $L = \lambda/\sqrt{2}$, $R = 110$ nm and $h = 4.0$ nm). (b) The ratio of dielectric permittivities $\varepsilon_{th}/\varepsilon_{num}$ as a function of ratio R/h, where ε_{th} is given by the Eq. (1), and ε_{num} is the silver permittivity extracted from [8].

An array of transversally orientated dimers can reflect an incident beam in -1st diffraction order, giving rise to anomalous reflection in a negative way. For example, at $\lambda = 440$ nm, $L = \lambda/\sqrt{2}$ and $\theta = 45^\circ$ the optimal parameters $h = 4.0$ nm, $R = 110$ nm provide reflection in counter-propagating direction with efficiency 86%, see Fig. 3(c). The near-zone electric field distribution is shown in the Fig. 3(d) and it indicates that this effect occurs when the lowest order longitudinal modes in dimers are excited, that corresponds to electric dipole oscillations. The dipole moment is directed along the inter-particle axis. Note that the efficiency is nearly constant for incident angle θ ranging from 35° to 60°, see Fig. 4(a). The optimal geometrical parameters and resulting efficiencies of the beam redirection for different λ are given in Table 1.

Table 1. The optimal geometrical parameters which provide the highest efficiency for the anomaly transmission and reflection in the lowest part of visible spectrum.

	Anomaly Transmission			Anomaly Reflection		
λ, nm	R, nm	h, nm	Eff., %	R, nm	h, nm	Eff., %
400	46	3.6	67.4	96	6.8	78.8
410	47.5	2.9	68.5	100	5.9	80.8
420	50	2.5	70.3	103	5.0	83.1
430	52	2.2	73.1	107	4.5	85.7
440	53	1.9	73.5	110	4.0	86.5
450	55	1.7	73.5	113	3.7	87.2
460	57	1.5	71.6	116	3.3	86.9
470	58	1.3	69.7	119	3.0	86.6
480	60	1.2	69.2	122	2.8	86.9
490	62	1.1	69.3	125	2.6	87.5
500	64	1.0	69.1	128	2.4	87.8

#251351 Received 5 Oct 2015; revised 12 Nov 2015; accepted 12 Nov 2015; published 18 Nov 2015

4. Discussion

In practice, fabrication of the pairs of silver cylinders with surface separation of just a few nanometers may be a challenging task. To increase the allowable separation one can change the shape of metallic particles. The idea is to fulfill resonance condition for larger values of the parameter h. Physically, the resonance condition for closely spaced particles enables the existence of standing surface plasmon waves in approximately flat region of the gap. Under the approximation it can be written as $\varepsilon_m/\varepsilon_d \sim -l/h$ for the lowest plasmonic mode, where l is the length of flat region [11]. Indeed, in the case of cylinders $l \sim \sqrt{Rh}$ and one obtains an estimate $\varepsilon_m/\varepsilon_d \approx -\sqrt{R/h}$, which is in agreement with Eq. (1) at $h \ll R$. The length l of the flat region can be increased by introducing the dimers consisting of metal rods with quasi-square cross section, see Fig. 2 (c). The length of square's side is equal to $2R$ and the corner radius is equal to r. The separation between metallic particles as previously is denoted by h.

Now the optimal parameters for $\lambda = 440$ nm depend on the ratio r/R, which defines the length of the flat region. In the case $r/R = 3/4$ the optimal parameters $R = 45$ nm and $h = 6.1$ nm ($R = 103$ nm and $h = 7.2$ nm) provide negative-angle refraction (reflection) with the efficiency 69% (82.9%). By reducing the ratio r/R one can further increase the gap separation h, however the efficiency will decrease: in the case $r/R = 1/2$ the optimal parameters $R = 42$ nm and $h = 10.5$ nm ($R = 97$ nm, $h = 11.2$ nm) provide only the efficiency 63% (79.4%). As always one has to find a compromise between large gap h and high efficiency of the scheme.

The other point is that fabricated cylinders have a finite length Λ and this may affect the resonance frequency. As it was shown in [13], the effect is negligible already at the cylinder's aspect ratio $\Lambda/2R = 4$. Thus, for discussed parameters the main limitation on the length stems from the transverse size of incident light beam, which should be smaller than the length of the cylinders. In the paper [6] the negative transmission phenomenon was experimentally demonstrated for the nanoposts with the length $\Lambda \approx 3\lambda$.

5. Conclusion

We have demonstrated that the periodic array of silver dimers (with carefully adjusted geometrical parameters) provides an anomalous reflection and refraction for impinging light in the lowest part of visible spectrum. The extraordinary optical response arises due to the excitation of the plasmonic resonances in the nanoscale gaps between particles constituting the dimers. Fig. 4(b) represents the ratio $\varepsilon_{th}/\varepsilon_{num}$ as a function of R/h. Here ε_{th} denotes the theoretical prediction (1) for the resonance metal permittivity of the lowest plasmonic modes of dimer, while ε_{num} is the metal permittivity corresponding to phenomena of anomalous refraction or reflection in numerics. It is easy to see that anomalous beam bending occurs at permittivity which is estimated by (1) up to the pre-factor of order of unity, $\varepsilon_{num} \approx 1.2\varepsilon_{th}$. We believe that deviation from the formula (1) is related mainly to interaction between neighbouring dimers. Note that (1) allows to estimate only the ratio R/h, while the optimal values of R and h by themselves cannot be derived within the quasi-electrostatic approximation.

Acknowledgments

Analytical part of the work was supported by RFBR grant No.14-02-31357, numerical simulations were carried under support of Russian grant No.MK-7373.2015.2 using Supercomputing Center of the Novosibirsk State University.

#251351 Received 5 Oct 2015; revised 12 Nov 2015; accepted 12 Nov 2015; published 18 Nov 2015